https://dx.doi.org/10.4314/ijs.v25i3.10

ESTIMATION OF AQUIFER PARAMETERS FROM ELECTRICAL RESISTIVITY DATA AND LITHOLOGS IN IDAH AREA, NORTHERN ANAMBRA BASIN, NIGERIA

Obasi, A. I.[1,*], Aigbadon, G. O.[1], Chinyem, F. I.[2], Chukwu, C. N.[3], Ahmed II, J. B.[1], Abubakar, S. O.[1], Attah, F. D.[1] and Akudo, E. O.[1]

[1]Department of Geology, Federal University Lokoja, P.M.B. 1154, Kogi State, Nigeria.
[2]Department of Geology, Faculty of Science, Delta State University, PMB 1, Abraka, Delta State, Nigeria.
[3]Department of Geology, Alex Ekwueme Federal University Ndufu-Alike Ikwo, Ebonyi State, Nigeria.
[*]Corresponding Author's Email: ikenna.obasi@fulokoja.edu.ng; obaik123@yahoo.com
(Received: 7th July, 2023; Accepted: 16th October, 2023)

ABSTRACT

The parameters of the aquifers in Idah area were characterized by integrating resistivity and litholog data. To achieve this, a total of twenty-three (23) Soundings were conducted by applying the 1-D Schlumberger resistivity array and integrating it with borehole lithologs to empirically determine the aquifer parameters in the Idah area, Northern Anambra Basin, Nigeria. The results of the analyses indicate that the aquifer zone resistivity ranges from 36.65 – 2065.31 Ωm while the aquifer thickness is between 15.60 m and 66.66 m. Its values of the longitudinal conductance (*S*), transverse resistance (*TR*), and hydraulic conductivity (*k*) are 0.01-1.13 mhos, 1518.90-90265.88 Ωm^2, and 0.31-13.44 m/day, respectively. The transmissivity (*T*) values vary from 4.88 to 557.78 m^2/day. T is inversely proportional to TR with a correlation coefficient of 0.28. The result of the reflection coefficient is in the range of -0.79 to 0.66, while that of the fractured contrast is between 0.11 and 5.06. The results suggest that an aquifer system that is predominantly fracture-based is underlying the region. Lithification and diagenesis influence the hydrological properties. The northern–central portions of the map are more suitable for groundwater exploration/exploitation than the southern/eastern ends.

Keywords: Anambra Basin, Idah, VES, Aquifer Parameters, Dar-Zarrouk Parameters.

INTRODUCTION

The evaluation of aquifer parameters contributes immensely to understanding the potential groundwater occurrence in a given environment and the effect of pumping on the aquifer system. In the absence of some primary geo-hydraulic data, such as the pumping test, some aquifer properties like the hydraulic conductivity (k) and transmissivity (T) that are very important in groundwater resource management can be obtained using Dar-Zarouk's equations (i.e. longitudinal conductance (S) and transverse resistance (TR)) (Ezeh, 2011; Raji 2014; Raji and Abdulkadir, 2020).

Based on simplicity and cost-effectiveness, a one-dimensional (1-D) resistivity survey employing the VES configuration is assumed to be a much more suitable approach in many geological settings for groundwater investigation (El-Hussaini *et al.* 1995; Ebong *et al.*, 2014; Obasi *et al.*, 2021). The method has also been found suitable to contribute substantially towards estimating aquifer parameters and can reduce the rate of pumping test and its cost implication as mentioned earlier.

The choice of Idah for this study was aimed at hydrodynamically characterizing the aquifer system in the area by correlating resistivity-derived aquifer parameters with their pumping test derived counterparts from a few existing boreholes in the same location. In this study, an attempt was made to estimate aquifer parameters by monitoring the variations of the groundwater resistivity within the area of investigation. The lithology of the subsurface layers, aquifer characteristics, geoelectric parameters, as well as hydrologic properties of the study area have been determined using the Vertical Electrical Sounding survey method. The sedimentary successions in the Northern Anambra Basin lack the primary porosity necessary for the occurrence of groundwater in many locations, hence, the need to investigate and locate areas affected by secondary porosity (fractured and weathered zones) becomes crucial.

LOCATION OF STUDY AND GEOLOGICAL SETTING

The study area lies within latitude 07°4'00" N and 07°9'00" N, and longitude 06°43'30" E and 06°45'00" E (Figure 1). It can be accessed using a combination of roads (both major and minor) and footpaths which are interconnected through the villages.

Geologically, the area is part of the sedimentary pile in the northern Anambra Basin. The basin is an inland basin that was formed due to the folding of the Abakaliki-Benue belt into the "Abakaliki Anticlinorium" (Murat, 1972) during the Santonian epeirogenic phase, and led to the formation of the Anambra and Afikpo basins in the northwest and southeast sides of the Abakaliki fold belt respectively (Burke, 1972). The basin is a unique lithostratigraphic entity that overlies the southern Benue Trough while itself is made up of the Campanian – Early Paleocene lithofacies and underlies the Niger Delta Basin in its southern reaches. Its basinal fill corresponds to the facies of the Nkporo Group and the Coal Measures that was described by Nwajide (2013). The Coal Measures include the Mamu and Nsukka Formations. The Idah area is part of the Mamu Formation in the Northern Anambra Basin and consists of carbonaceous shales, mudstone, clay, coals, sandstone, and siltstone. Being a product of an anoxic setting, the sandstone facies of this unit are ferruginized and consolidated. Hence, they seem to lack primary porosity in many locations. Since the primary porosity is lacking, the fractured and weathered zones became very relevant for groundwater occurrence.

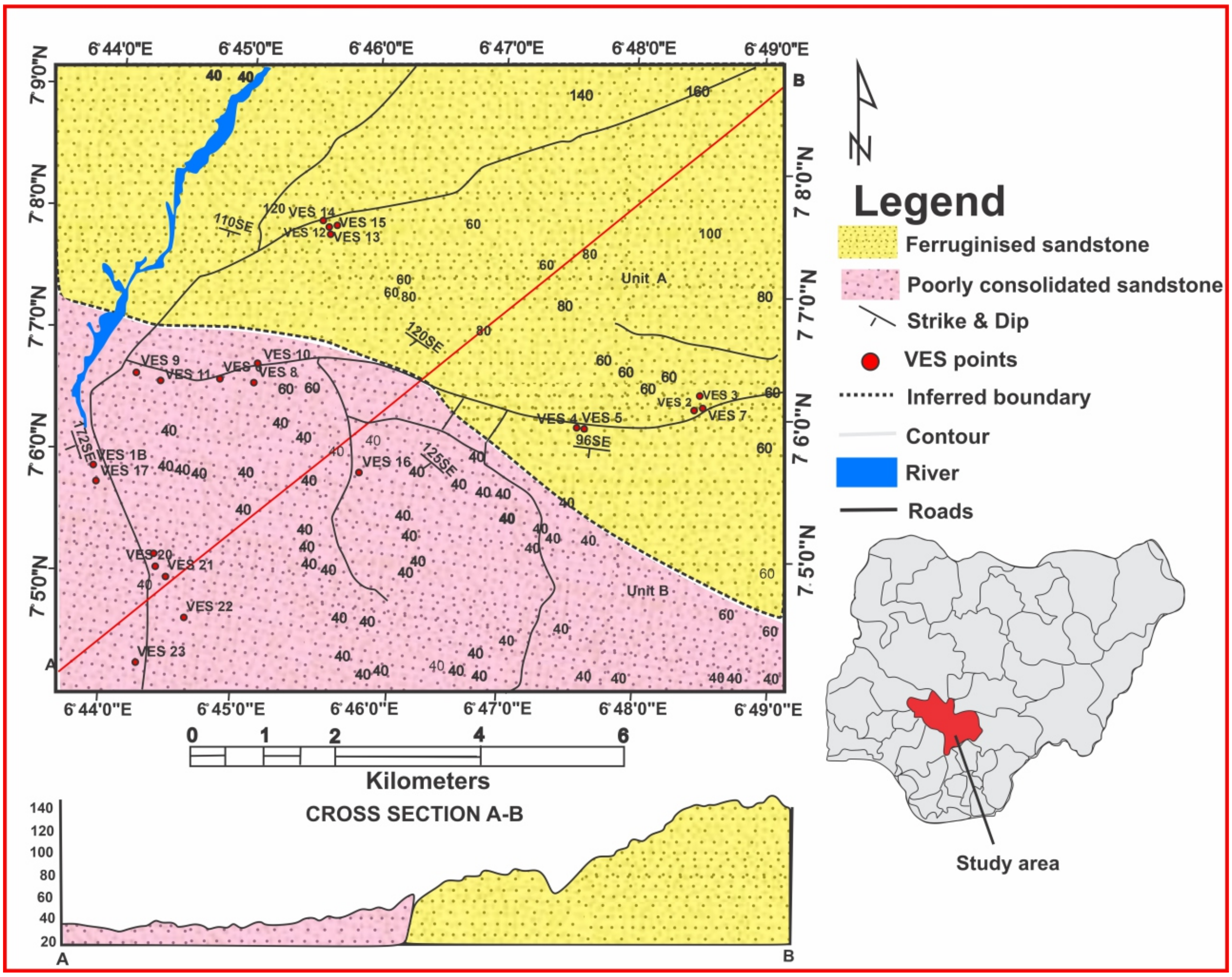

Figure 1: The Geological map of Idah area with VES points, River, and cross-section.

MATERIALS AND METHODS

The Schlumberger array of the electrical resistivity method was applied in conducting a 1-D resistivity survey in twenty-three (23) locations within the Idah area using a current electrode spread in the range of 1-150 m and a potential electrode spread of 0.25-20 m. For simplicity of geo-referencing, the spatial distribution of each surveyed point was established using the Global Positioning System (GPS). To ensure data quality, the resistance measured and computed resistivities were manually plotted on the field against the relevant current ($^{AB}/_2$) electrode separation. When a curve showed anomaly peaks in comparison to earlier survey points, the data acquisition was repeated to eliminate doubts and/or uncertainties. At the end of the fieldwork, a graph of the apparent resistivity values against current electrode spacing (AB) was plotted on the bi-logarithmic coordinates with the help of the Interpex IX1Dv.3.38 modeling software (Interpex, 2004) to be able to generate geoelectric layers (Figure 2).

(a)

(b)

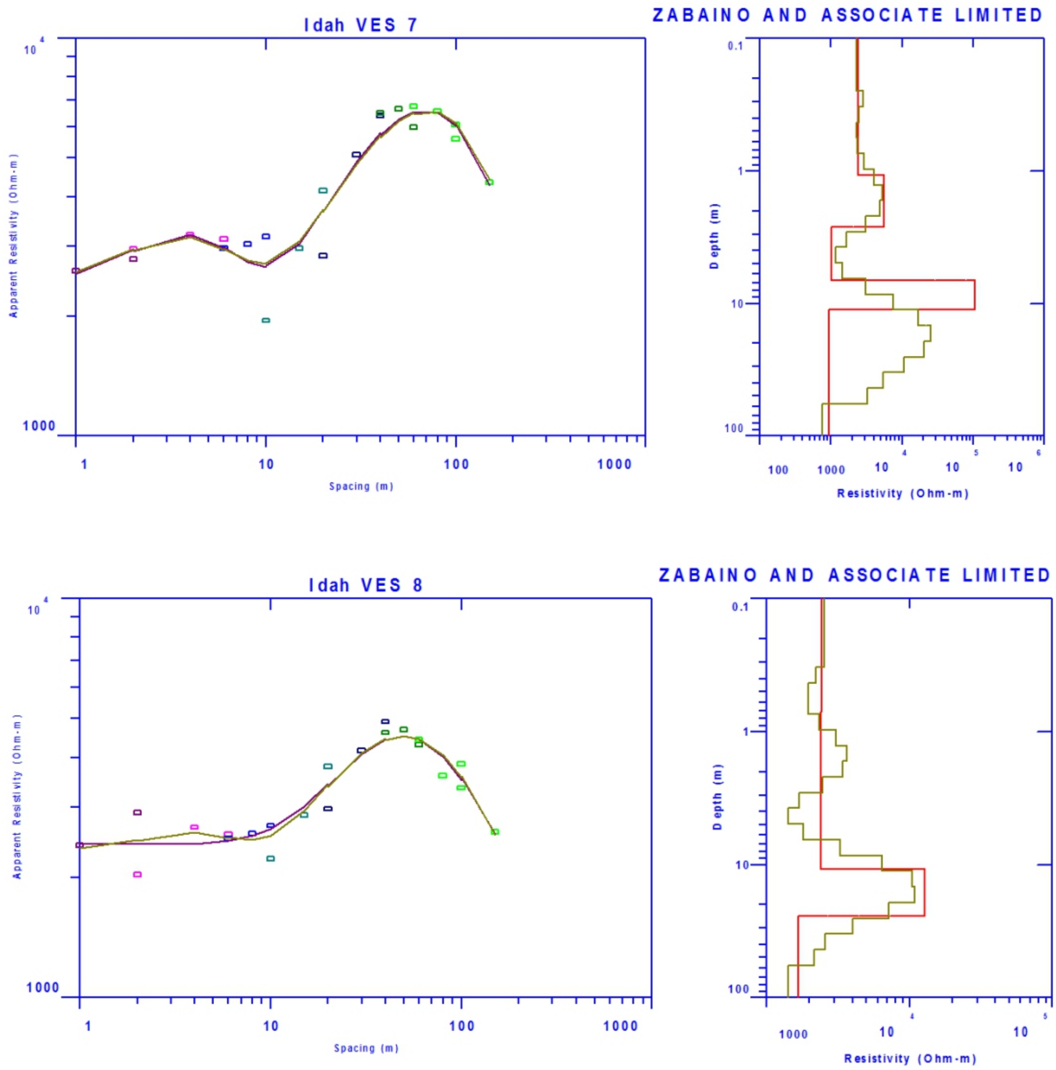

Figure 2: Samples of the VES curves in the Idah area (a - VES graph 7, b - VES graph 8).

Equations 1 and 2 were applied in the calculation of the Dar-Zarouk parameters (Salem, 1999), and the aquifer parameters were calculated using Equations 3, 4, 5, and 6, respectively (Raji and Abdulkadir, 2020). In generating the lithologic logs (Lithologs), the Logging While Drilling (LWD) approach was employed, during the drilling of 14 boreholes, using rock cuttings from the boreholes. The modeling of the spatial distribution of the derived aquifer properties and 2D spatial maps was carried out with the aid of ArcGIS 10.7.1 software, while the IBM SPSS statistics 26 software aided the correlation of the different data sets.

Longitudinal conductance, $S = \sum_{i-1}^{N} \frac{h_i}{\rho_i}$ (1)

Where h_i is the aquifer thickness, while ρ_i is the aquifer resistivity.

Transverse resistance, $TR = \sum_{i-1}^{N} h_i \times \rho_i$ (2)

Hydraulic conductivity, $K = 386.40 R_{rw}^{-0.93283}$ (3)

Where R_{rw} is the aquifer resistivity

Transmissivity, $T = K.h$ (4)

Reflection coefficient, $R_C = \frac{\rho_n - \rho_{n-1}}{\rho_n + \rho_{n-1}}$ (5)

Fractured contrast, $F_C = \frac{\rho_n}{\rho_{n-1}}$ (6)

Where ρ_n is the apparent resistivity of a geo-electric layer, h_w is the thickness of the aquifer zone, and ρ_{n-1} is the apparent resistivity of the geo-electric layer overlying the nth layer.

RESULTS AND DISCUSSION

The results of the analyses as shown in Table 1 indicate two to six geoelectric layers. These layers correspond to four geologic units and have been interpreted as topsoil, clays, shales, and sandstones. The variation in layer characteristics is attributable to differences in the degree of weathering and fracture anisotropy (Oli *et al.*, 2022).

The resistivity of the aquiferous zone (ρ_i) ranges from about 36.65 – 2065.31 Ωm (Figure 3a and Table 2). The aquifer resistivity map shows low resistivity around the central – southwestern portions of the map, with the highest resistivity occurring in the northern part. The geologic map of the area (Figure 1) indicates that the oldest rocks occur in the northern portion and comprise highly consolidated, ferruginized sandstones. Hence, the occurrence of the highest resistivity values in the northern part of the study area is in agreement with the subsurface geology. The direction of the dip of the host rocks suggests that the rocks are younging southwestwards. This coincided with the least resistivity values encountered in the southwest portion of the map. Consequently, the resistivity range for the aquifer in the northern portion of the location of study is higher than its counterpart towards the southern portion of the map due to the age and depth of burial, and their associated post-depositional processes comprising lithification and diagenesis. Hence, the aquifer zone's resistivity is a function of the underlying geology. In areas that are underlain by shales and poorly consolidated sandstones, their resistivity values are much lower than their older and highly consolidated counterparts (Obasi *et al.*, 2021). The very low aquifer resistivity values could imply the presence of some shally/weathered/regolith aquiferous zones with possible clay effects (Salem, 2001a; Obasi *et al.*, 2021).

Table 1: Geoelectric data from the study area.

VES	LAT.	LONG.	LOCATION NAME	ρ_1(Ωm)	ρ_2(Ωm)	ρ_3(Ωm)	ρ_4(Ωm)	ρ_5(Ωm)	h_1(m)	h_2(m)	h_3(m)	h_4(m)
1	7.11	6.81	Comm. Sec. Sch, Ogbogbo	609.45	10.47	1584.20	-	-	1.43	70.63	-	-
2	7.10	6.81	Comm. Sec. Sch., Ogbogbo	785.81	338.58	20.79	472.34	7.75	0.68	2.60	24.31	79.57
3	7.10	6.81	After Comm. Sec. Sch. Ogbogbo	1516.90	420.07	58.07	-	-	0.48	1.96	-	-
4	7.10	6.79	Iyegu, Idah	4034.60	319.17	11463.00	-	-	3.10	1.96	-	-
5	7.10	6.79	Iyegu, Idah	223.21	3669.50	395.26	842.70	-	1.15	1.66	48.34	-
6	7.11	6.75	Idah Sec. Commercial College	1305.70	27005.00	2103.40	-	-	0.58	0.36	-	-
7	7.11	6.75	Idah Sec. Commercial College	2442.30	5660.80	1025.50	0.11	932.53	1.09	1.55	4.07	4.37
8	7.11	6.75	Idah Sec. Commercial College	2444.20	2404.90	12751.00	1671.00	-	0.71	10.06	13.68	-
9	7.11	6.75	Idah Sec. Commercial College	3490.10	8107.70	9935.40	1352.80	-	1.35	10.03	11.26	-
10	7.11	6.75	Idah Sec. Commercial College	1050.80	7.79	11630.00	906.95	0.40	0.40	0.39	1.90	-
11	7.11	6.74	Stadium, Idah	1840.90	3711.50	1530.90	0.12	-	0.85	8.27	48.21	-
12	7.13	6.76	Technical College Idah 1	884.35	7871.40	2064.60	-	-	0.91	2.06	-	-
13	7.13	6.76	Technical College Idah 2	2322.50	5110.80	676.12	58701.00	10149.00	2.14	3.16	12.10	95.56
14	7.13	6.76	Technical College Idah 3	816.38	0.18	707.53	0.34	-	1.15	0.44	5.83	-
15	7.13	6.76	Technical College Idah 4	772.36	68262.00	527.60	6114.00	12895.00	0.18	0.65	2.00	3.51
16	7.13	6.30	Ichekene River Bank	124.62	108.94	-	-	-	3.91	-	-	-
17	7.10	6.73	Ichekene close to Ibaji	28.07	12711.00	2553.11	7.97	106.97	0.17	0.83	0.38	1.60
18	7.10	6.73	Ichekene River Bank	50.07	220.43	170.34	27217.00	70.56	0.76	0.21	36.34	36.89
19	7.09	6.74	Close to Ibaji road, Ichekene	14.85	3033.50	20.61	87.47	-	0.17	1.41	4.02	-
20	7.08	6.74	Opposite Ibaji road, Ichekene	19.19	4.15	302.77	-	-	5.04	2.32	-	-
21	7.08	6.74	Ibaji road, Ichekene	34.95	63.02	-	-	-	1.58	-	-	-
22	7.08	6.74	Ibaji road, Ichekene	8.64	36.64	-	-	-	1.78	-	-	-
23	7.07	6.73	Ibaji road, Ichekene	104.94	9.15	269.29	-	-	2.85	0.97	-	-

Table 2: Estimated aquifer parameters in the study area.

VES No.	**Latitude**	**Longitude**	ρ_{aq}**(Ωm)**	$h_{a\,(m)}$	S**(mhos)**	TR **(Ωm^2)**	**Rw$^{-0.93283}$**	k **(m/day)**	T **(m^2/day)**	ρ_{n-1} **(Ωm)**	R_c	F_c
1	7.106194	6.807917	1584.20	27.94	0.02	44262.55	0.001	0.40	11.18	309.96	0.67	5.11
2	7.10475	6.808194	472.34	49.30	0.10	23286.36	0.003	1.24	60.99	381.73	0.11	1.24
4	7.10175	6.792556	319.17	29.69	0.09	9476.16	0.005	1.78	52.94	2176.89	-0.74	0.15
5	7.102056	6.791639	395.26	32.00	0.08	12648.32	0.004	1.46	46.75	1429.32	-0.57	0.28
7	7.107806	6.748556	827.71	43.40	0.05	35922.61	0.002	0.73	31.82	3042.87	-0.57	0.27
8	7.108167	6.74975	1786.50	42.50	0.02	75926.25	0.001	0.36	15.20	2424.55	-0.15	0.74
9	7.109583	6.750417	1352.80	67.10	0.05	90772.88	0.001	0.46	31.11	5721.50	-0.62	0.24
11	7.1085	6.737333	1412.90	24.20	0.02	34192.18	0.001	0.45	10.77	2361.10	-0.25	0.60
12	7.129667	6.758611	2065.50	15.60	0.01	32221.80	0.001	0.31	4.87	3606.78	-0.27	0.57
16	7.129528	6.29972	108.94	61.50	0.56	6699.81	0.013	4.86	298.93	116.78	-0.03	0.93
19	7.085556	6.736333	87.47	18.80	0.21	1644.44	0.015	5.97	112.14	789.11	-0.80	0.11
21	7.082389	6.737778	63.02	42.00	0.67	2646.84	0.021	8.10	340.16	48.99	0.13	1.29
22	7.082556	6.740361	36.60	41.50	1.13	1518.90	0.035	13.45	557.99	22.64	0.24	1.62
23	7.071	6.734056	269.29	33.98	0.13	9150.47	0.005	2.09	71.00	127.79	0.36	2.11

(a)

(b)

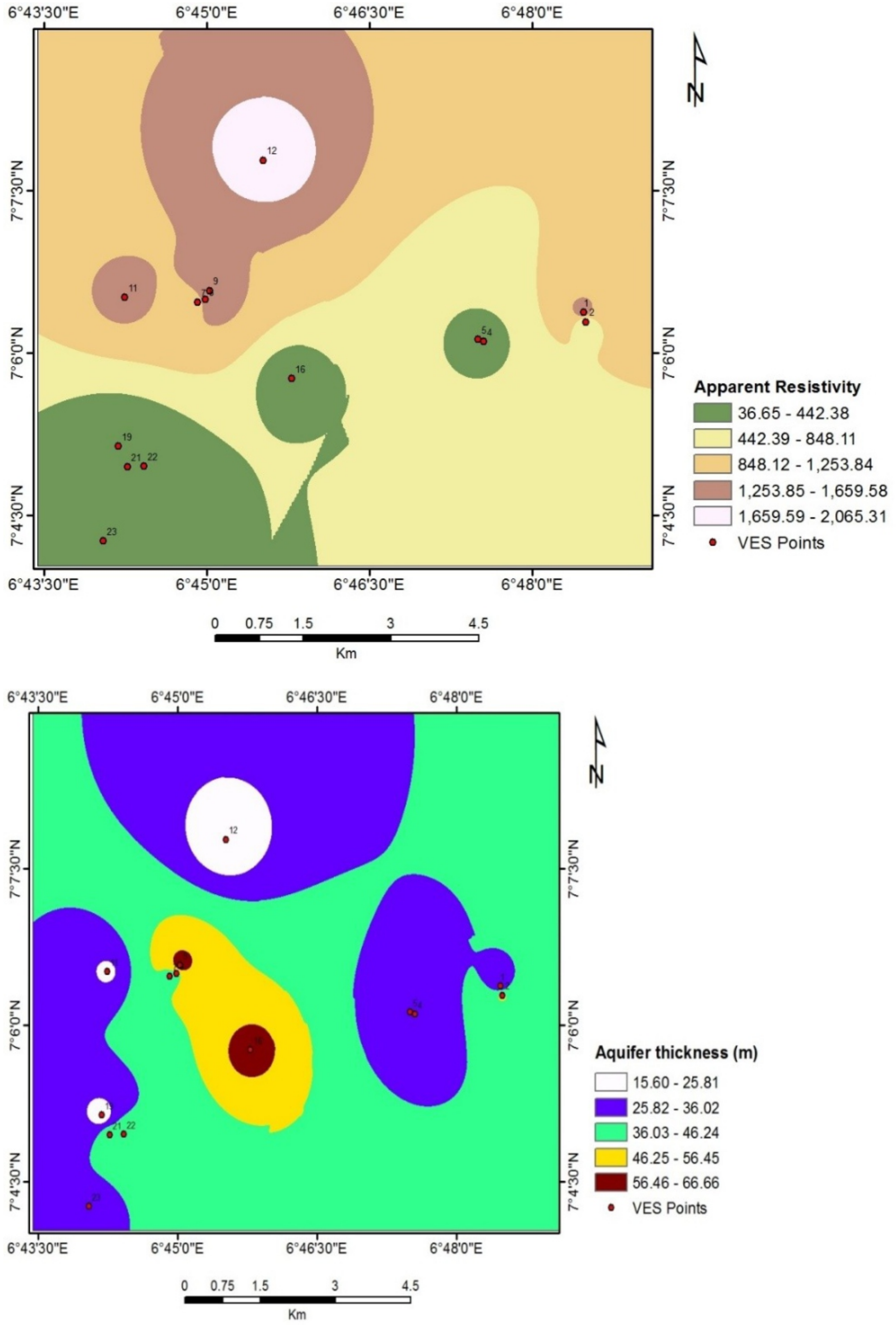

Figure 3: Maps of aquifer resistivity and thickness in Idah (a - aquifer resistivity map, b - aquifer thickness map).

The rock type, pore-water resistivity, physical parameters, and lithological characteristics are among the factors that have a significant influence on aquifer resistivity (Salem, 2001a; Salem, 2001b). The degree of water saturation could also influence aquifer zone resistivity (Uhlemann *et al.*, 2017). Hence, the low resistivity in the Southwest part of the study location could also imply higher aquifer saturation in that region (Obasi *et al.*, 2023). The aquifer thickness (Figure 3b) did not follow a definite pattern as the aquifer resistivity. The highest thickness (⩾ 56 m) occurred almost at the central portion while the least thickness (⩽ 16 m) occurred across all the portions of the map.

The values of the *S* (Figure 4a) range from 0.01-1.13 mhos in the study area. The *S* is approximately inversely proportional to ρ_i values, with the least values of *S* occurring in the northern portion of the map, while the value increases southwards. This is an indication of electric anisotropy in which there is more parallel current flow across the bedding planes of the sedimentary rocks than perpendicular to the beds (Salem, 1994). The oldest ferruginized sandstone aquifers in the northern portion of the map have the least *S* values due to the absence of clays in the aquiferous zone (Salem, 1994). Hence, the anisotropy, in this case, is more in favour of the vertical current flow than the horizontal flow.

The result of the transverse resistance (*TR*) (Table 2 and Figure 4b) shows that the lowest values (≤ 1.52) occurred in the Southwestern portion of Idah. The bulk of the area has moderate TR values. The highest *TR* values (≥ 90) were observed in the older sandstone unit. This is a further indication of the significant impact of lithification and diagenesis on the resistivity of rocks, as well as the absence of clay (Salem, 1994) within the aquifers in the ferruginized sandstone unit.

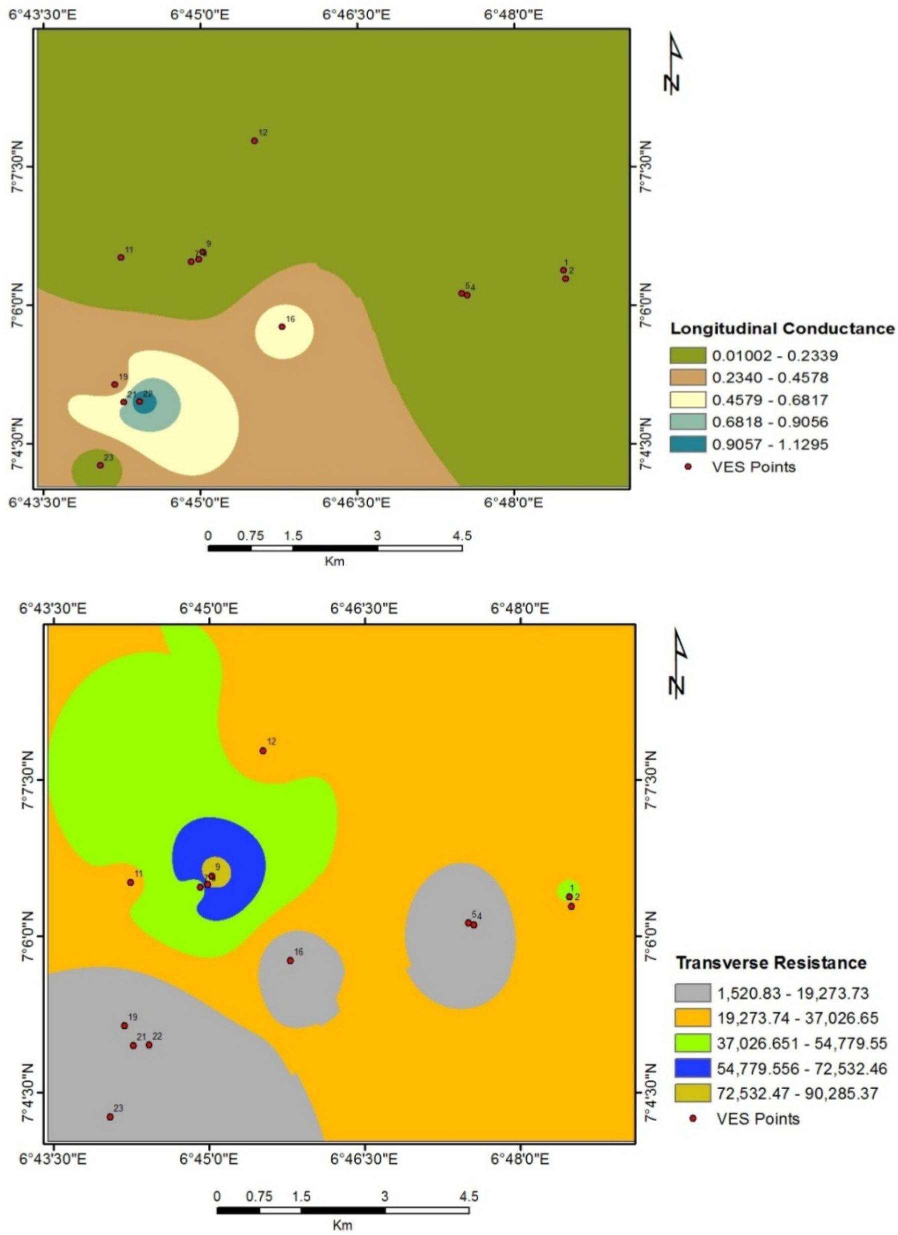

Figure 4: Aquifer Dar-Zarouk parameters in Idah. (a - map of the longitudinal conductance, b - map of transverse resistance)

The result of the hydraulic conductivity (k) (Figure 5) shows that the k is least in the older rock units and increases towards the youngest rock unit in the direction of the dip. The very low k values encountered in the sandstone units suggest that they host post-depositional secondary aquiferous units either in the form of weathered-regolith, fractures, or faults (Hitchmough *et al.*, 2007; Nastev *et al.*, 2008; Obiora *et al.*, 2016) and not syn-depositional primary aquifer system arising from poor consolidation of sediments. Although the entire Anambra basin is not known for any key tectonic event (Nwajide, 2013), field studies revealed that the sandstone unit in the area is highly consolidated and ferruginized. Structural elements that are capable of aiding migration and hosting fluids within the region have been previously identified (Dim *et al.*, 2017, 2019). The above information is suggestive that groundwater occurrence and permeability in the study area are dependent on the presence and interconnectivity of fractures. The highest k values (VES 21 and 22) were encountered in shale aquifers (Obasi *et al.*, 2021). Contrary to the fact that clay mineral occurrence in the aquifer system is popular for lowering the aquifer's hydraulic conductivity (Salem, 1999; Ebong *et al.*, 2014), the shaly aquifer understudy has higher k values than the sandstone aquifer. This indicates that the occurrence of groundwater and its distribution in the entire area of study is a function of geospatial existence in the interconnectivity of fractures. Where there is a wider fracture or interconnectivity of fractures, the aquifer permeability and transmissivity will increase (Obasi *et al.*, 2021).

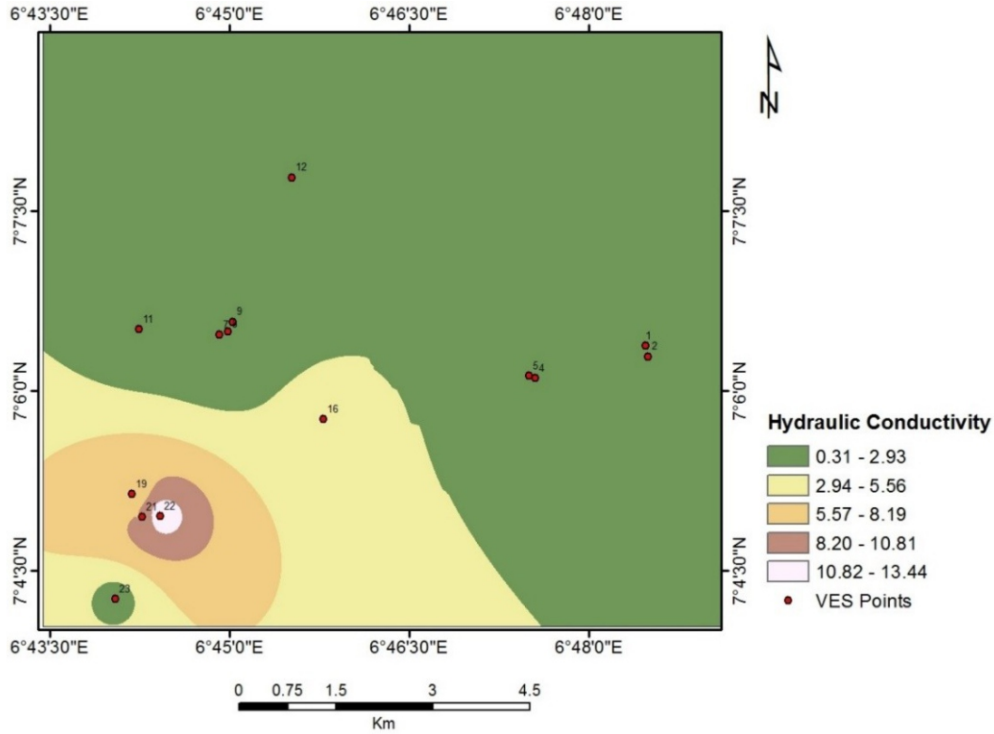

Figure 5: The hydraulic conductivity map of the study area.

The transmissivity (T) map of Idah (Figure 6a) indicates that it ranges from 4.88 – 557.78 m^2/day. The T is directly proportional to k. Areas with high water-bearing capacity are associated with high T (Obiora *et al.*, 2016). T correlates inversely with TR (Figure 6b) with a linear correlation coefficient of 0.28, suggesting a discontinuous flow in some parts of the study area (Salem, 2001b; Ebong *et al.*, 2014).

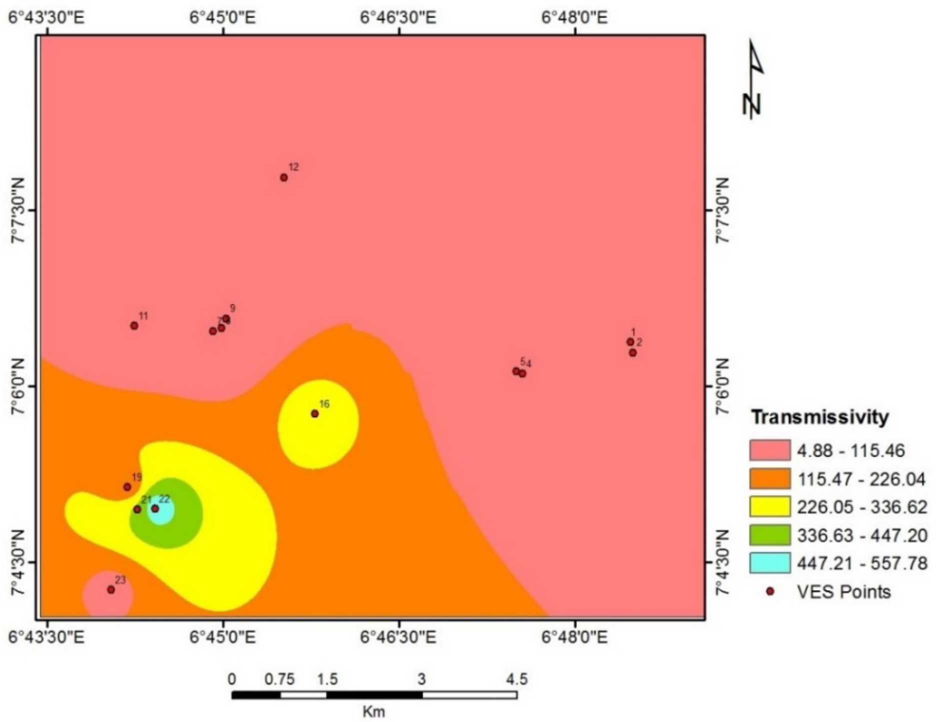

Figure 6a: Transmissivity map of the study area.

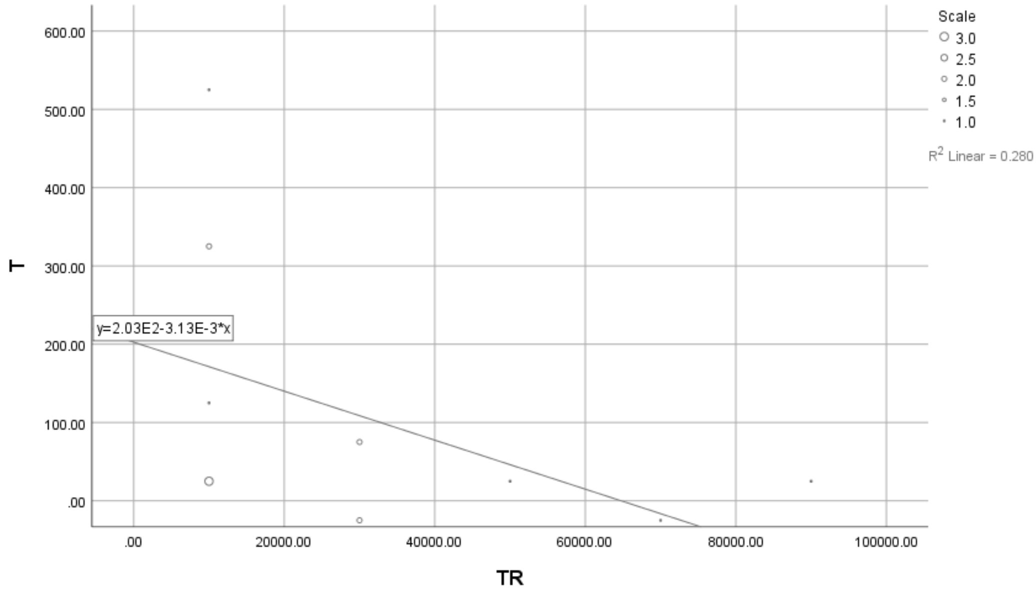

Figure 6b: A correlation of T and TR in the study area.

The results of the reflection coefficient and fracture contrast analyses in Idah area are presented in Figures 7a and 7b, respectively. The lowest values (≤ -0.79) occurred in the central-northern portion of the area. Both parameters followed the same trend, with their highest values (0.66 and 5.06) occurring at the eastern and southern ends of the map. Low values of the parameters are associated with the presence of a high quantity of water within the aquiferous unit (Olayinka *et al*., 2000; Raji and AbdulKaldir, 2020). Based on the results of the R_c and F_c, the ferruginized sandstone unit at the northern portion of the map has a higher density of water-filled fractures than its younger, poorly consolidated sandstone counterpart.

(a)

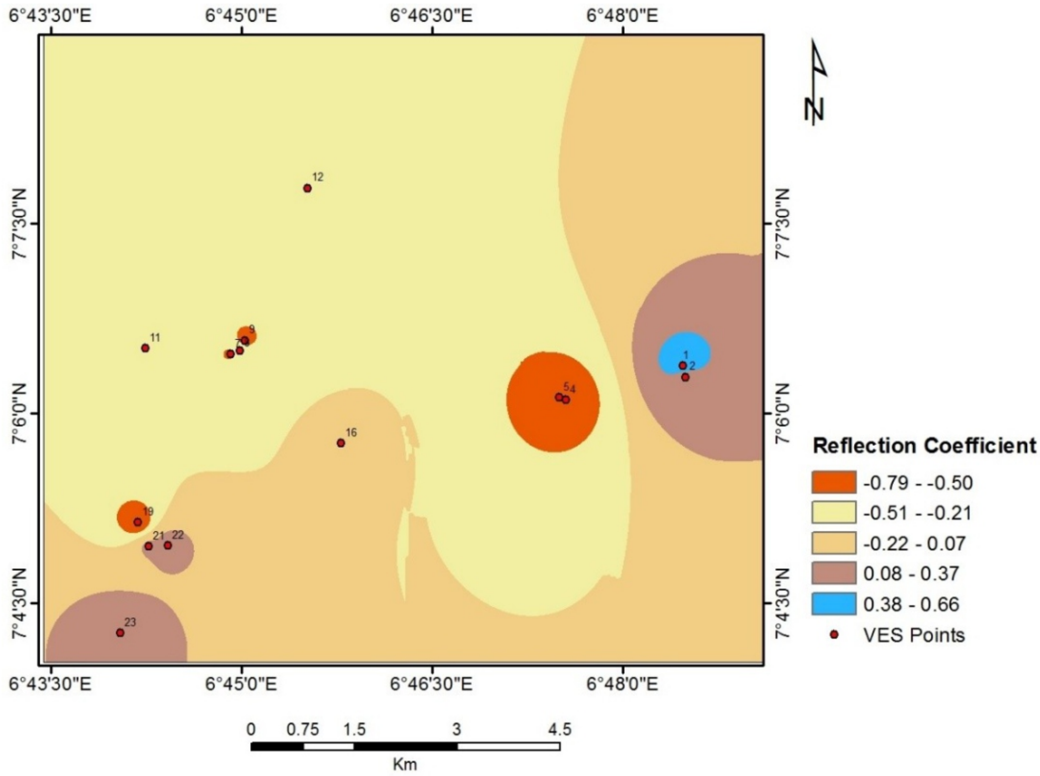

(b)

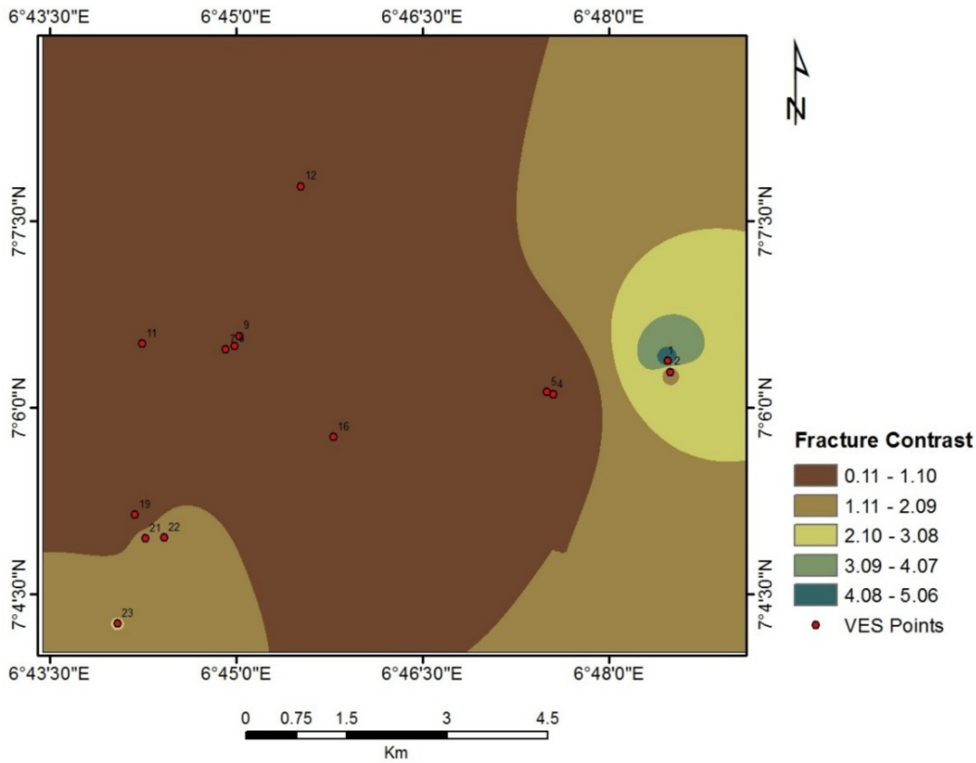

Figure 7: Maps of (a) reflection coefficient and (b) fracture contrast in the study area.

CONCLUSION

In this study, the characterization of the subsurface geoelectric parameters for estimating aquifers in the Idah area, Northern Anambra Basin was made with the aid of 1-D electrical resistivity data. The interpreted VES data showed that the aquifer parameters are a result of lithification and diagenetic alteration, which therefore, made the older rocks have better aquifer properties than the younger rocks. From the interpretations made, the area has low-moderate values of the aquifer properties and could be associated with fractured-rock aquifers. The northern–central portion of the Idah area has shown more prospective for groundwater exploration than the southern–eastern ends of the study area.

CONFLICT OF INTEREST

To the best of the knowledge of the authors, there is no conflict of interest in this article. The opinions offered in this article are purely research-oriented and devoid of any form of bias.

AUTHORS' CONTRIBUTION

All the authors contributed immensely to the production of this manuscript, although not in equal proportion. While every author participated in drafting the original manuscript, O.A.I. and G.O.A. handled the final proofreading. J.B.A. and F.I.C. produced all the maps, and C.N.C., S.O.A. and F.D.A. typed the manuscript, while E.O.A. handled the statistical analysis.

REFERENCES

Burke, K. C., Dessauvagie, T. F. J. and Whiteman, A. J., 1972. Opening of the Gulf of Guinea and geological history of the Benue Depression and Niger delta. *Nat. Phys. Sci.* 233:51–55.

Dim, C. I. P., Mode, A. Y. and Okwara, I. C., 2019. Signatures of key petroleum system elements: outcrop examples from the Anambra Basin, Southeastern Nigeria. *Journal of Petroleum Exploration and Production Technology* 9:1615–1631. doi: 10.1007/s13202-018-0589-2

Dim, C. I. P., Onuoha, K. M., Okeugo, C. G. and Ozumba, B. M., 2017. Petroleum system elements within the Late Cretaceous and early Paleogene sediments of Nigeria's inland basins: An integrated sequence stratigraphic approach. *Journal of African Earth Sciences*, 130:76–86. doi: 10.1016/j.jafrearsci.2017.03.007

Ebong, D. E., Akpan, A. E. and Onwuegbuche, A. A., 2014. Estimation of geohydraulic parameters from fractured shales and sandstone aquifers of Abi (Nigeria) using electrical resistivity and hydrogeologic measurements. *J. Afr. Earth Sci.* 96:99–109. doi: 10.1016/j.jafrearsci.2014.03.026

El-Hussaini, A. H., Ibrahim, H. A. and Bakhelt, A. A., 1995. Interpretation of geoelectrical data from an area of the entrance of Wadi Qena, eastern Desert, Egypt. *J King Saudi Univ.* 7:257–276.

Ezeh, C. C., 2011. Geoelectrical studies for estimating aquifer hydraulic properties in Enugu State, Nigeria. *Int. J. Phys. Sci.* 6(14):3319–3329. doi: 10.5897/IJPS10.274

Heigold, P. C., Gilkeson, R. H., Cartwright, K. and Reed, P. C., 1979. Aquifer Transmissivity from surfacial Electrical methods. *Groundwater*, 17 (4):338–345.

Hitchmough, A. M., Riley, M. S., Herbert, A. W. and Tellam, J. H., 2007. Estimating the hydraulic properties of the fracture network in a sandstone aquifer. *Journal of Contaminant Hydrology,* 93: 38–57.

Interpex, 2004. IX1Dv.3.38–1D Inversion software, Interpex Limited, Golden, Colorado, USA(www.interpex.com).

Maillet, R., 1947. The fundamental equations of electrical prospecting. *Geophysics*, 12(4): 529–556. doi: 10.1190/1.1437342

Murat, R. C., 1972. Stratigraphy and palaeogeography of the cretaceous and lower tertiary in Southern Nigeria. In: Dessauvagie, F.J., Whiteman, A.J. (Eds.), African Geology. University of Ibadan Press, Ibadan, Nigeria, pp. 251-266.

Nastev, M., Morin, R. H., Godin, R. and Rouleau, A., 2008. "Developing conceptual hydrogeological model for Potsdam sandstones in southwestern Quebec, Canada". *Hydrogeology Journal*, 16: 373–388 doi: 10.1007/s10040-007-0267-9

Nwajide, C. S., 2013. Geology of Nigeria's Sedimentary Basins, CSS Bookshops Ltd, Lagos Nigeria. 451p.

Obasi, A. I., Onwa, N. M. and Ezekiel, O. I., 2021. Application of the resistivity method in characterizing fractured aquifer in sedimentary rocks in Abakaliki area, southern Benue Trough, Nigeria. *Envi. Earth Sci.*, 80:24. doi: 10.1007/s12665-020-09303-w

Obasi A. I., Ahmed II J. B., Anakwuba E. K., Aigbadon G. O., Akudo E. O., and Onwa N. M., 2023. Assessment of aquifer vulnerability in fractured rocks in the Abakaliki area, southeastern Nigeria, using geophysical and geological data. *Envi. Earth Sci.*, 82:171. doi: 10.1007/s12665-023-10851-0

Obiora, D. N., Ibuoti, J. C. and George, N. J., 2016. Evaluation of Aquifer Potential, Geoelectric and Hydraulic Parameters in Ezza North, Southeastern Nigeria, using Geoelectric Sounding. *Int. J. Environ. Sci. Technol.,* 13:435–444. doi: 10.1007/s1376 2-015-0886-y

Olayinka, A. I., Obere, F. O. and David, L. M., 2000. Estimation of Longitudinal Resistivity from Schlumberger Sounding Curves. *J. Min. Geol.*, 36(2):225–242.

Oli, I. C., Opara, A. I., Okeke, O. C., Akaolisa, C. Z., Akakuru, O. C., Osi-Okeke, I. and Udeh, H. M., 2022. Evaluation of aquifer hydraulic conductivity and transmissivity of Ezza/Ikwo area, Southeastern Nigeria, using pumping test and surficial resistivity techniques. Environ Monit. Assess. 194:719. doi: 10.1007/s10661-022-10341-z

Raji, W. O. and Abdulkadir, K. A., 2020. Evaluation of groundwater potential of bedrock aquifers in Geological Sheet 223 Ilorin, Nigeria, using geo-electric sounding. *Appli. Water Sci.*, 10:220. doi: 10.1007/s13201-020-01303-2

Raji, W. O., 2014. Review of electrical and gravity methods of near surface exploration for groundwater. *Nigerian J. Technol. Dev.* 11(2):31–38.

Salem, H. S., 1994. The electric and hydraulic anisotropic behavior of the Jeanne d'Arc Basin reservoirs. *Journal of Petroleum Science and Engineering*, 12(1): 49–66.

Salem, H. S., 1999. Determination of fluid transmissivity and electric transverse resistance for shallow aquifers and deep reservoirs from surface and well-log electric measurements. *Hydrology and Earth System Sciences*, 3(3): 421–427.

Salem, H. S., 2001a. The influence of clay conductivity on electric measurements of glacial aquifers. *Energy Sources, Part A: Recovery, Utilization, and Environmental Effects*, 23(3): 225–234.

Salem, H. S., 2001b. Modeling of lithology and hydraulic conductivity of shallow sediments from resistivity measurements, using Schlumberger vertical electric soundings. Energy Sources, Part A: Recovery, Utilization, and Environmental Effects, 23(7): 599–618. doi: 10.1080/00908310152004719

Tizro, A. T., Voudouris, K. S., Salchzade, M. and Mashayekhi, H., 2010. Hydrogeological framework and estimation of aquifer hydraulic parameter using geoelectrical data: a case study from West Iran. *Hydrogeol. J.*, 18:917–929.

Uhlemann, S., J. Chambers, P. Wilkinson, H. Maurer, A. Merritt, P. Meldrum, O. Kuras, D. Gunn, A. Smith, and T. Dijkstra (2017), Four-dimensional imaging of moisture dynamics during landslide reactivation. *J. Geophys. Res. Earth Surf.,* 122:398–418. doi:10.1002/ 2016JF003983.

Vchery, A. and Hobbs, B., 2003. Resistivity imaging to determine clay cover and permeable units at an ex-industrial site. *Near Surf Geophys.*, 1:21–30.